Bioscience Reports (2023) **43** BSR20231348
https://doi.org/10.1042/BSR20231348

PORTLAND PRESS

Research Article

The presence of a G-quadruplex prone sequence upstream of a minimal promoter increases transcriptional activity in the yeast *Saccharomyces cerevisiae*

Libuše Kratochvilová[1,2,*], Matúš Vojsovič[1,2,*], Natália Valková[1], Lucie Šislerová[1,2], Zeinab El Rashed[3], Alberto Inga[4], Paola Monti[5,†] and Václav Brázda[1,2,†]

[1]Institute of Biophysics of the Czech Academy of Sciences, Královopolská 135, 61200 Brno, Czech Republic; [2]Department of Food Chemistry and Biotechnology, Faculty of Chemistry, Brno University of Technology, Purkyňova 118, 61200 Brno, Czech Republic; [3]Gene Expression Regulation SSD, IRCCS Ospedale Policlinico San Martino, 16132 Genoa, Italy; [4]Laboratory of Transcriptional Networks, Department of Cellular, Computational and Integrative Biology, CIBIO, University of Trento, via Sommarive 9, 38123 Trento, Italy; [5]Mutagenesis and Cancer Prevention UO, IRCCS Ospedale Policlinico San Martino, 16132 Genoa, Italy

Correspondence: Václav Brázda (vaclav@ibp.cz)

Non-canonical secondary structures in DNA are increasingly being revealed as critical players in DNA metabolism, including modulating the accessibility and activity of promoters. These structures comprise the so-called G-quadruplexes (G4s) that are formed from sequences rich in guanine bases. Using a well-defined transcriptional reporter system, we sought to systematically investigate the impact of the presence of G4 structures on transcription in yeast *Saccharomyces cerevisiae*. To this aim, different G4 prone sequences were modeled to vary the chance of intramolecular G4 formation, analyzed *in vitro* by Thioflavin T binding test and circular dichroism and then placed at the yeast *ADE2* locus on chromosome XV, downstream and adjacent to a P53 response element (RE) and upstream from a minimal *CYC1* promoter and Luciferase 1 (*LUC1*) reporter gene in isogenic strains. While the minimal *CYC1* promoter provides basal reporter activity, the P53 RE enables *LUC1* transactivation under the control of P53 family proteins expressed under the inducible *GAL1* promoter. Thus, the impact of the different G4 prone sequences on both basal and P53 family protein-dependent expression was measured after shifting cells onto galactose containing medium. The results showed that the presence of G4 prone sequences upstream of a yeast minimal promoter increased its basal activity proportionally to their potential to form intramolecular G4 structures; consequently, this feature, when present near the target binding site of P53 family transcription factors, can be exploited to regulate the transcriptional activity of P53, P63 and P73 proteins.

[*]These authors contributed equally.
[†]These authors are last co-authors.

Received: 08 August 2023
Revised: 07 November 2023
Accepted: 21 November 2023

Accepted Manuscript online: 21 November 2023
Version of Record published: 19 December 2023

Introduction

Although the shape of the DNA molecule is primarily epitomized in the double helix, the ENCODE project has shown that DNA can form noncanonical secondary structures with biological significance [1]. These structures include the so-called G-quadruplexes (G4s) that are formed from sequences rich in guanine bases. G4s are constituted of four guanine bases arranged in a square planar conformation (G-tetrad) held together by Hoogsteen hydrogen bonding and further stabilized by potassium or sodium ions [2,3]. G4s can be presented in various topologies including antiparallel, parallel, and hybrid structures, depending on the relative orientation of the DNA strand within the structure; intermolecular G4 structures can also be formed when more than one DNA strand creates the final structure [4]. G4s have been shown to be

Bioscience Reports (2023) **43** BSR20231348
https://doi.org/10.1042/BSR20231348

involved in processes such as DNA replication, gene transcription, translation, and the maintenance of genome stability; they occur in specific sequences such as telomeres and promoter regions of oncogenes, and also on 5′ and 3′ untranslated regions (UTRs) of mRNAs [2,5,6]. Interestingly, bioinformatics analysis of the binding sites of several transcription factors showed their potential to interact with G4s [6,7] and provided the basis for the assumption that positive or negative regulations occur between transcription factors and G4 structures [8]. Moreover, the increased frequency of G4 motifs in gene promoters compared with the rest of the genome suggests a significant contribution to the regulation of the expression of those genes [9]. Experiments carried out with a single chain antibody specific for G4 structures showed the involvement of G4s not only during the initiation of transcription, but also during its termination [8]. The first verified evidence of G4s influence on gene expression was demonstrated for the *MYC* oncogene, where mutations of a G4 in the promoter region affected *MYC* expression *in vivo* [10,11]. Subsequent studies addressed the regulation of transcription through G4 ligands (e.g., TMPyP4 and many others), resulting in a comparable decrease in transcription of *MYC* [11], *KRAS* [12] and *KIT* [13] oncogenes. Therefore, G4 targeting is suggested for cancer therapy [14,15].

The P53 family of transcription factors comprises the structurally related P53, P63, and P73 proteins that share an N-terminal transactivation domain (TA), a central sequence-specific DNA-binding domain (DBD) and an oligomerization domain (OD) at the C-terminus. All three proteins act mainly as tetramers to induce expression of a plethora of target genes involved in different cellular pathways, including cell proliferation, apoptosis, DNA repair, angiogenesis, metabolism and differentiation [16–18]. The three family members are also characterized by similar gene structures that produce groups of mRNAs controlled by separate promoters and encoding proteins with alternative N-terminal regions [19,20]. While the variants generated from the distal promoter contain the complete TA domain (TA-isoforms) and are transactivation competent, those generated from internal promoters lack the full TA domain (ΔN-isoforms) but still bind DNA, showing both specific transactivation ability and dominant negative activity. To further complicate the P53 family landscape, the transcripts are also subject to alternative splicing of the 3′ portion, giving rise to a combinatorial variety of P53, P63 and P73 specific isoforms [21,22].

Transcriptional regulation by P53 family proteins is mainly achieved through binding to a degenerate DNA motif known as the P53 response element (RE), consisting of two decameric half-sites separated by a short spacer (RRRCWWGYYY-n-RRRCWWGYYY, where R stands for a purine, W for A/T, Y for a pyrimidine and n for spacer) [23,24]. However, while the binding affinities of P53 family transcription factors are related to the primary sequence features of the RE, other factors that can modulate binding and transactivation are related to DNA accessibility within chromatin and to various features of the so-called indirect-readouts or shape-readouts; these are dependent on DNA structural features that can be influenced by trans-factors including proteins, non-coding RNAs and epigenetic changes that impact nucleosome density and positioning [24].

Interestingly, local unfolding events within the DNA double helix are able to stimulate the formation of G4 structures, potentially contributing to orchestrate P53 family cell-type specific transcriptomes [25]. Based on the critical role of these DNA structural elements in the modulation of transcriptional activity, we previously evaluated the influence of a G4 prone sequence from KSHV (Kaposi sarcoma-associated herpes virus) in proximity to a P53 RE from the *BBC3* (PUMA) target gene on the transactivation potential of ΔN- and TA-variants of P53 family α isoforms [25,26]. Here, by using the same yeast-based assay, we study the effect of different G4 prone sequences on both basal and P53 family dependent expression of the Luciferase 1 reporter gene (*LUC1*). To this aim, different G4 prone sequences were modeled to vary the chance of intramolecular G4 formation and studied *in vitro* for the different propensity of forming G4 structures by Thioflavin T binding and circular dichroism analyses. The sequences were then placed downstream and adjacent from the PUMA RE, constructing otherwise isogenic yeast reporter strains. The impact of various G4 prone sequences was measured after transforming cells with centromeric inducible expression vectors and shifting them to galactose-containing medium to modulate the levels of P53, P63, and P73 (wild-type TA α isoforms). The results highlight that a higher propensity to form G4 structures upstream of the promoter correlates with higher transcriptional activity of both basal and transcription factor-dependent levels.

Material and methods

Synthetic oligonucleotides

Synthetic oligonucleotides were purchased from Sigma-Aldrich and diluted with ultrapure water to a final concentration of 100 μM (Table 1). The PUMA sequence was derived from the *BBC3* (PUMA) P53 target gene; oligonucleotide sequences with different G4 formation potential were designed to decrease the chance of intramolecular G4 formation by mutating the KSHV G-quadruplex sequence [25]. KSHV-Mut2.0 and KSHV-Mut1.5 sequences were designed by the G4 Killer program [27] to change G4 Hunter score below 2.0 and 1.5, respectively; the sequences of KSHV-1NO,

Table 1 Oligonucleotides used in the present study

Oligonucleotides	Sequence	G4 Hunter score
PUMA	5′-CTGCAAGTCCTGACTTGTCC-3′	−0.350
KSHV	5′-GGGGCGGGGGACGGGGGAGGGG-3′	3.182
KSHV-1NO	5′-GAAGCGGGGGACGGGGGAGGGG-3′	2.545
KSHV-2NO	5′-GAAGCGAAAGACGGGGGAGGGG-3′	1.727
KSHV-Mut2.0	5′-GGAGCGGTGGACGGTGGAGGGG-3′	1.591
KSHV-Mut1.5	5′- GAGCGGTGGACGGTGGAGGAG-3′	1.091
KSHV-3NO	5′- AAGCGAAAGACGAAAGAGGGG-3′	0.909

KSHV-2NO and KSHV-3NO were designed by sequential substitution of G bases in guanine repeats. The propensities of G4 formation were predicted for these sequences by the G4 Hunter program and measured as G4 Hunter scores (Table 1) [28].

Thioflavin T assay analysis

The thioflavin T (ThT) binding test was performed according to the procedure described in [29]. Synthetic oligonucleotides at a final concentration of 2 μM in 100 mM Tris-HCl (pH 7.5) or 100 mM Tris-HCl (pH 7.5) containing 100 mM KCl were denatured (95°C for 5 min) and gradually cooled to room temperature. Oligonucleotides were mixed with ThT in a 2:1 molar ratio and measured in a 384-well titration microplate reader at room temperature in three replicates (excitation at 425 nm). Fluorescence emission was detected at 490 nm; the measured fluorescence intensities of individual oligonucleotides were compared to the fluorescence intensity of the buffer with ThT without DNA (I/I_0).

Circular dichroism spectroscopy analysis

Synthetic oligonucleotides at final concentration 3 μM in 10 mM Tris-HCl or 10 mM Tris-HCl containing 100 mM KCl were denatured (95°C for 5 min) and gradually cooled to room temperature. Circular Dichroism (CD) allows characterization of the topology of the resulting secondary structure by comparison with model spectra [30,31]. Spectra were measured on a Jasco 815 dichrograph in 1 cm tapered quartz cuvettes that were placed in a thermostatically controlled holder at 20°C. Four scans of each sample were taken at a scan rate of 100 nm · min^{-1} with a data pitch of 0.5 nm in the wavelength range 200–330 nm, averaged, and the resulting spectra were smoothed using the Savitzky-Golay smoothing algorithm with a 15-point window. The CD signal was expressed as the difference in the molar absorption coefficient $\Delta\varepsilon$ of the left- and right-hand polarized light. CD measurements were taken also after 24 h.

Yeast reporter strains, plasmids and manipulations

Saccharomyces cerevisiae reporter strains that contain, in addition to the P53 RE from the *BBC3* (PUMA) target gene (5′-CTGCAAGTCCTGACTTGTCC-3′), different G4 prone sequences (Table 1), were already available [25] or newly created by the *Delitto Perfetto* approach [32]. G4 prone sequences were located downstream of the P53 RE and upstream of the minimal CYC1-derived promoter controlling the *LUC1* reporter gene, cloned at the yeast *ADE2* locus on chromosome XV [33] (see sequences and chromosomal locus description in Figure S1). The following isogenic yeast strains were used: yLFM-PUMA (PUMA), yLFM-PUMA-KSHV (P-K), yLFM-PUMA-KSHV-1NO (P-K-1NO), yLFM-PUMA-KSHV-2NO (P-K-2NO), yLFM-PUMA-KSHV-Mut2.0 (P-K-Mut2.0), yLFM-PUMA-KSHV-Mut1.5 (P-K-Mut1.5) and yLFM-PUMA-KSHV-3NO (P-K-3NO). Vectors based on pTSG plasmid containing the coding sequences for wild-type P53 family TA α isoforms (i.e., P53, P63, and P73) expressed under a yeast-inducible *GAL1,10* promoter were already available along with the empty vector pRS314 (*TRP1* selection marker) [34]. Yeast cells were transformed by the lithium acetate method as previously described [35]. Yeast transformants were selected on plates lacking tryptophan and containing high amounts of adenine (200 mg/l), given the deletion of the *ADE2* open reading frame and promoter in all strains, and incubated for 3 days at 30°C. Colonies were then patched onto the same selective plates to expand them prior to reporter assays.

Yeast luciferase assay

Yeast transformants (empty and wild-type P53 family TA α isoforms) were resuspended using a 96-well plate in tryptophan-selective liquid medium containing raffinose as carbon source and then diluted in selective media supplemented with galactose at final concentrations of 0.016% or 1%. The shift from glucose containing plates to raffinose

Bioscience Reports (2023) **43** BSR20231348
https://doi.org/10.1042/BSR20231348

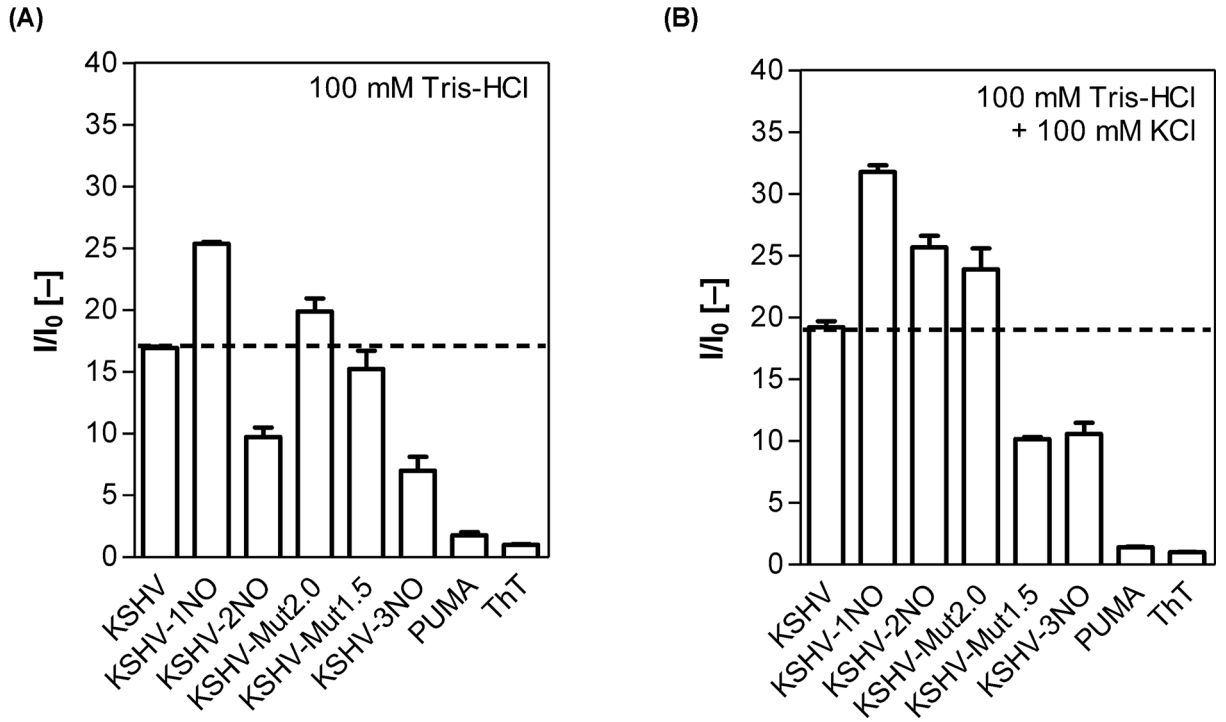

Figure 1. Evaluation of G4 formation potential *in vitro* by ThT assay

Oligonucleotides were hybridized in 100 mM HCl (**A**) or in the same buffer with the addition of 100 mM KCl (**B**). The $I_{(KCl)}/I_{(0)}$ fold values are reported in Supplementary Table S1.

plus galactose media causes dose-dependent activation of the *GAL1,10* promoter to induce P53 family protein expression at moderate and high levels [33]. Reporter expression is assayed after 6 h of incubation at 30°C. Luciferase assays were performed using a white 96-well plate, where 20 µl of yeast culture was mixed in each well with an equal volume of 2× Passive Lysis Buffer (Promega) to permeabilize cells by 15 min of shaking at room temperature; then the firefly luciferase substrate (20 µl) was added (Bright-Glo™ Luciferase Assay Kit, Promega). Light unit values were normalized to the OD_{600} value of each culture measured from the 96-well culture plates. Results were expressed by (i) relative light units (RLU, i.e., Firefly units/OD), (ii) fold changes using the RLU values obtained from transformants with the empty pRS314 vector as reference, and (iii) relative activities as ratio of fold change. At least three independent cultures were measured for each experiment,

Statistical analysis

Ordinary one-way ANOVA followed by comparisons test were performed using GraphPad Prism version 9 for Mac (GraphPad Software, San Diego, California, U.S.A.).

Results

Formation of G4s structures *in vitro*

First, we assessed G4 formation in the oligonucleotides under study (Table 1) using the ThT assay; as the G4 structure is stabilized by potassium ions, we used buffers with and without KCl addition. In both buffers, oligonucleotides with potential to form G4s achieved a fluorescence intensity several times higher than the PUMA oligonucleotide (negative control), whose fluorescence was only that of the ThT background signal value (Figure 1A,B and Supplementary Table S1); furthermore, fluorescent signals were higher in buffer with potassium ions (Figure 1A,B and Supplementary Table S1).

The ThT fluorescence for KSHV-1NO, KSHV-2NO and KSHV-3NO oligonucleotides decreased in accordance with the decrease of G4 Hunter score (Figure 1A,B and Supplementary Table S1); the increase in the fluorescent signal in the presence of potassium ions was most pronounced for the KSHV-2NO oligonucleotide, while the lowest increase was observed for KSHV-1NO. KSHV-3NO, characterized by the lowest G4 Hunter score, showed approximately 1.5

times higher fluorescence intensity in the presence of KCl compared with without KCl; this increase by a G4 sequence that is designed to strongly reduce the formation of the intramolecular G4 structure is probably associated with the ability of potassium ions to facilitate the formation of intermolecular G-quadruplex structures.

KSHV-Mut2.0 and KSHV-Mut1.5 oligonucleotides showed comparable fluorescence intensity in buffer without potassium ions (Figure 1A and Supplementary Table S1). A higher fluorescence intensity in KCl-containing medium was achieved only by KSHV-Mut2.0, which confirmed the formation and stabilization of G4 structures; conversely, KSHV-Mut1.5 showed a decrease in signal, with a value comparable with KSHV-3NO (Figure 1B and Supplementary Table S1). This result may suggest a destabilization of the emerging G4 structures or the formation of different loops through the contribution of electrostatic interactions with a less stable conformation.

Next, we characterized G-quadruplex formation using CD spectroscopy; measurements were also taken after 24 h to determine changes in conformation over time (Figure 2 and Supplementary Figure S2). PUMA oligonucleotide spectra (Figure 2A) did not show any typical peaks for G4 even after the addition of potassium ions, as apparent from the absence of the G4 characteristic peak in the 210 nm region [36]; moreover, the spectra were nearly identical in both types of buffers, reaching positive peaks at 220 and 280 nm and a negative peak at 250 nm. Similarly, KSHV-3NO with the lowest G4 Hunter score (0.909) did not form a G4 structure even in the presence of potassium ions (Figure 2G). In contrast with PUMA and KSHV-3NO oligonucleotides, the KSHV sequence showed characteristics typical for a parallel G-quadruplex, with positive peaks at 210 and 260 nm and a negative peak at 240 nm; moreover, a small peak around 295 nm suggested that mixed or antiparallel G4 structures were also possible for this sequence (Figure 2B). The strong formation of G4 structures in the KSHV sequence was also supported by the presence of the typical peaks described above in the absence of potassium ions.

The spectra of KSHV-1NO (Figure 2E) and KSHV-2NO (Figure 2F) suggested that these sequences could form parallel G4 structures, especially in buffer containing potassium ions. The CD spectra of KSHV-Mut2.0 (Figure 2C) and KSHV-Mut1.5 (Figure 2D) reached positive peaks around 216 and 264 nm and a negative peak at 242 nm, indicating the possible presence of a parallel G4 structure without the addition of potassium ions; in potassium buffer, the latter oligonucleotide formed a hybrid G4 structure characterized by positive peaks around 210, 260 and 295 nm.

After 24 h, there was a slight increase in signal intensity without any change in topology for KSHV-1NO, KSHV-2NO, KSHV-Mut2.0 and KSHV-Mut1.5 in KCl buffer; for the remaining motifs, there was a decrease in signal and in some cases deviations in the measured spectra, but no evidence of a change in conformation with time (Supplementary Figure S2). Taken together, the results confirm the differential propensity of oligonucleotides we selected to form G4 structures *in vitro*, revealing consistency with their selection based on the G4 Hunter score.

Effect of the presence of G4 prone sequences on basal reporter activity in a yeast-based assay

The same panel of G4 prone sequences assayed *in vitro* were placed downstream and adjacent to P53 PUMA RE in isogenic yeast reporter strains and analyzed by a functional assay. We began by examining the impact of the sequences on the basal expression of the *LUC1* reporter 6 h after shifting the yeast cells to 0.016% and 1% galactose containing medium.

By plotting the RLU data and ordering the G4 prone sequences by decreasing G4 Hunter score, a proportional trend was observed. G4 prone sequences KSHV and KSHV-1NO led to higher transcription and this effect was progressively reduced by decreasing the strength of the G4 sequence measured by G4 Hunter (Figure 3), being partially affected also by the type of G4 prone motif. Indeed, transcription in P-K-1NO, P-K-2NO and P-K-3NO strains decreased; similarly, this effect was evident with P-K-Mut2.0 and P-K-Mut1.5 strains. However, the P-K-3NO strain, characterized by the lowest G4 Hunter score (0.909) did not show the lowest RLU value, and was statistically different from the PUMA control strain. Conversely, transcription in P-K-Mut1.5 strain (G4 Hunter score 1.091) was not or only weakly statistically different from PUMA at 0.016% and 1% galactose, respectively; finally, transcription in P-K and P-K-1NO strains was comparable and both were higher than the PUMA strain ($P<0.0001$).

These results suggested that the basal reporter transcription can be stimulated by the presence of a G4 sequence in *S. cerevisiae* in relation to the propensity to form G4 structures.

Effect of the presence of G4 prone sequences on transcription factor-dependent reporter activity

Next, we examined the potential impact of G4 prone sequences on transcription where sequence-specific transcription factors bind upstream of the promoter and the G4 site, stimulating *LUC1* reporter expression. We exploited wild-type human P53 family proteins (i.e., TA P53, P63 and P73 α isoforms) under an inducible promoter to obtain

Bioscience Reports (2023) **43** BSR20231348
https://doi.org/10.1042/BSR20231348

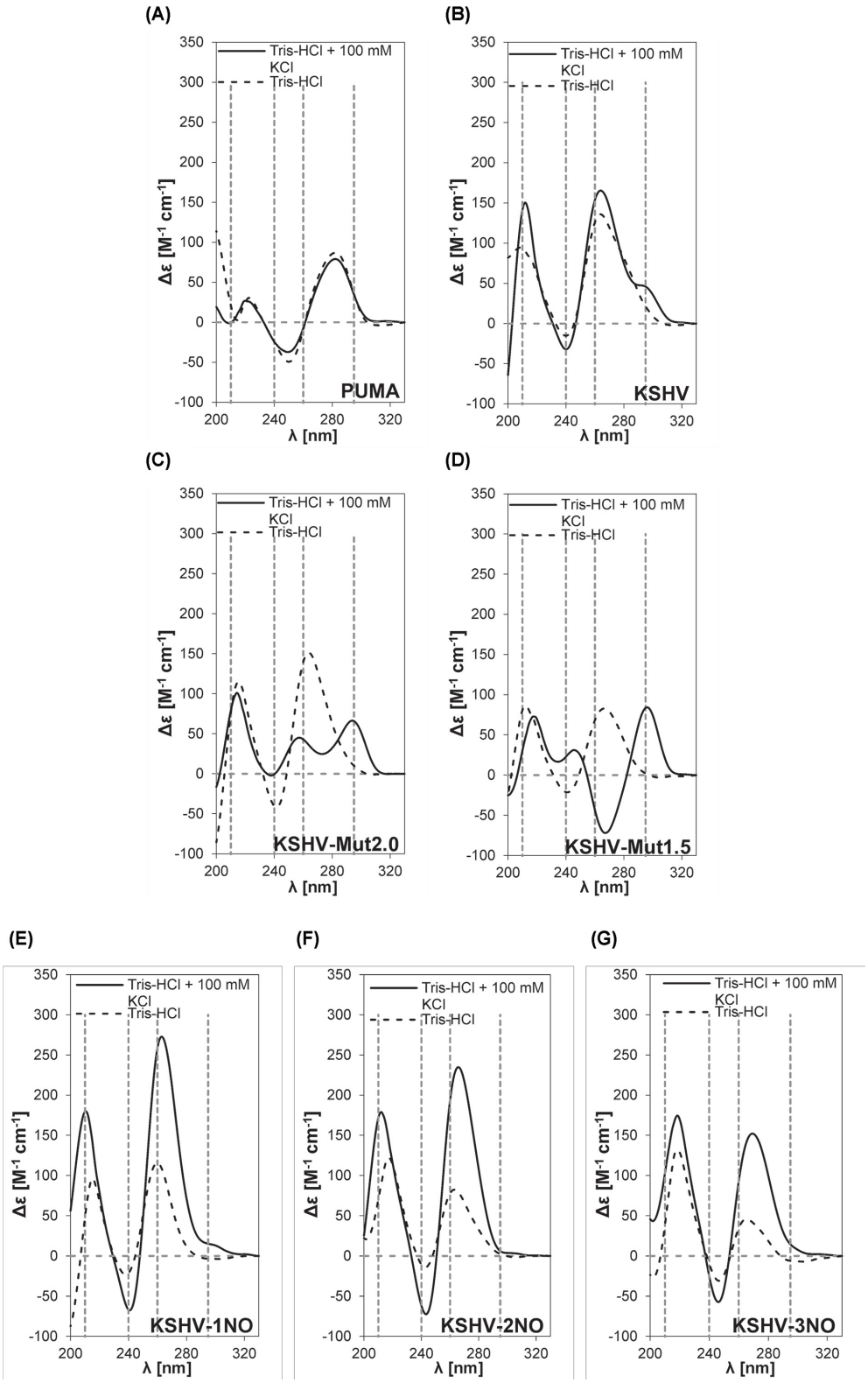

Figure 2. Evaluation of G4s formation potential *in vitro* by CD spectra analysis

CD spectra of oligonucleotides of (**A**) PUMA, (**B**) KSHV, (**C**) KSHV-Mut2.0, (**D**) KSHV-Mut1.5, (**E**) KSHV-1NO, (**F**) KSHV-2NO and (**G**) KSHV-3NO in medium without stabilizing potassium ions (dashed line) and in medium supplemented with 100 mM KCl (solid line). Wavelengths (210, 240, 260 and 295 nm) characteristic for the presence of G4 conformations in CD spectra are highlighted by gray dashed lines.

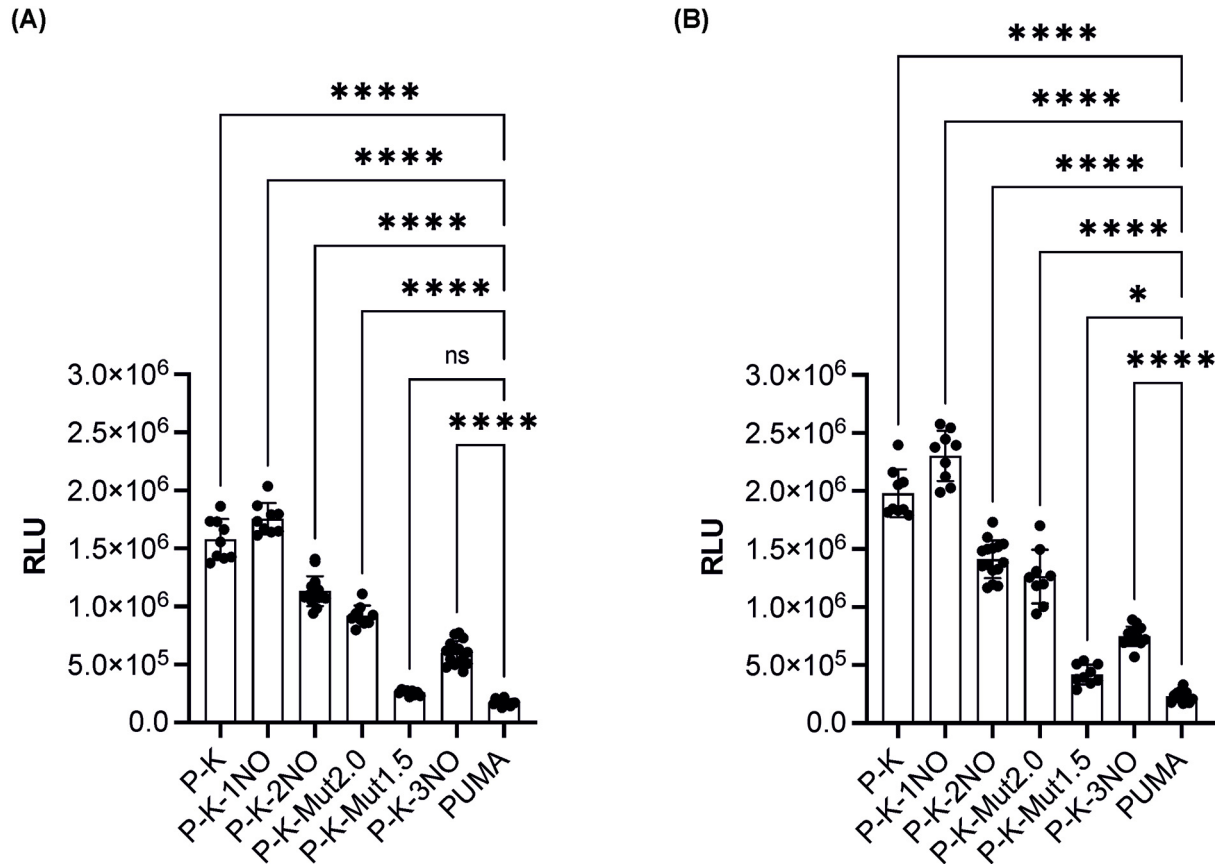

Figure 3. Effect of G4 prone sequences on basal reporter activity in the yeast *S. cerevisiae*

(**A**) *RLU measurements for the indicated panel of yLFM reporter strains from empty plasmid (pRS314) yeast transformants at 0.016% galactose for 6 h*. (**B**) *RLU measurements as above at 1% galactose*. Data are presented as mean ± standard deviation, (SD) of at least three biological replicates, and individual values are also plotted. The symbols * and **** indicate significant differences with P=0.0461 and P<0.0001, respectively between PUMA strain and those containing G4 regulatory elements. ns, not significant. Ordinary one-way ANOVA test.

moderate or high-level expression. As expected, *LUC1* was enhanced at the lower level of galactose inducer, especially by P53 protein with respect to basal transcription (Figure 4). The presence of G4 prone sequences with different scores had a weak effect on modulation of P53 transactivation (Figure 4A,D); conversely, a trend is present indicating that P63- and P73-dependent reporter transcription was stimulated by the presence of G4 sequences (Figure 4B,E: P63; Figure 4C,F: P73). Based on these results, we conclude that a strong transcription factor such as wild-type P53 is less influenced by G4 prone sequences compared to the weaker P63 and P73 proteins.

Then, by plotting the data as fold change, i.e., using the basal transactivation levels to normalize the impact of P53 family proteins expression in each strain, as previously done in our transactivation studies [25,26], lower fold change values for the G4-containing strains compared to the PUMA control were evident (Supplementary Figure S3). Overall, the results were consistent with the view that G4 prone sequences are associated with higher basal transcription, a feature that may favor the transactivation function of the weak transcription factors P63 and P73. This effect becomes more evident when focusing on the relative activity of P63 and P73 transcription factors with respect to P53 (Figure 5). In general, the presence of G4 sequences with higher score reduces the gap in transactivation between P53 and the other two family members P63 and P73.

Discussion

Transcription is regulated by several mechanisms, one of the most important being protein binding to promoters and enhancers [37]. Sequence-specific transcription factors interact with their target binding sites and their specificity and activity can be influenced by the presence of non-B and higher order DNA structures [38–41]. A prominent

Bioscience Reports (2023) **43** BSR20231348
https://doi.org/10.1042/BSR20231348

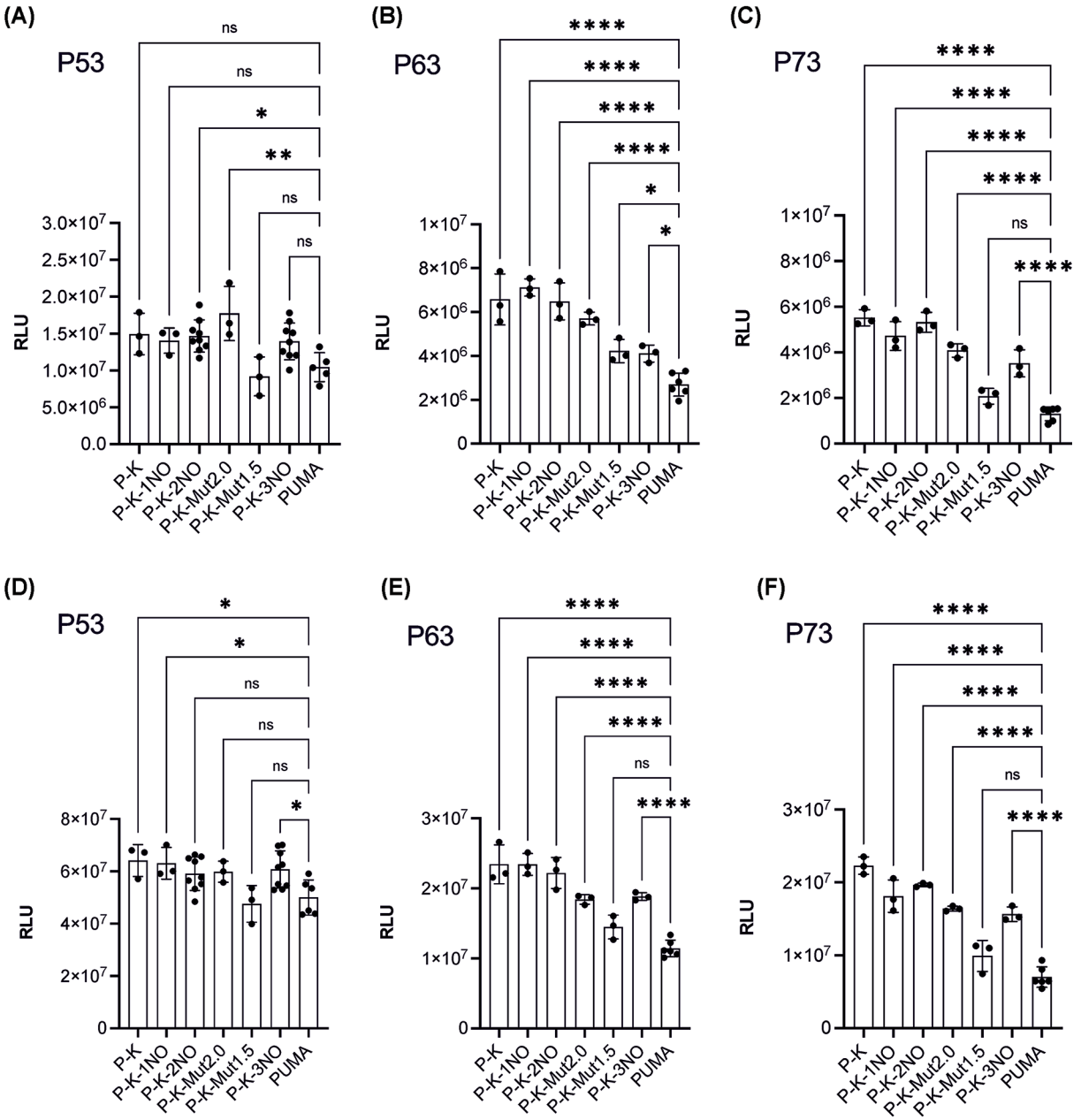

Figure 4. Effect of G4 prone sequences on P53 family-dependent reporter activity in the yeast *S. cerevisiae*

(**A–C**): *RLU measurements for the indicated panel of yLFM reporter strains expressing P53, P63 or P73 at 0.016% galactose for 6 h*. (**D–F**) *RLU measurements as above at 1% galactose for 6 h*. Data are presented as mean ± standard deviation (SD) of at least three biological replicates, and individual values are also plotted. The symbols *, ** and **** indicate significant differences with $P \leq 0.0406$, $P = 0.0017$ and $P < 0.0001$, respectively between PUMA strain and those containing G4 regulatory elements. ns, not significant. Ordinary one-way ANOVA test.

category of such structural elements includes DNA G-quadruplexes (G4s) consisting of secondary structures formed by stacked G-tetrads [9,42]. G4 prone sequences are present in all organisms including *S. cerevisiae* [43] and human [44–46]. Recently, G4 structures were confirmed and visualized within cells using conformation antibodies or small molecule ligands, and their presence has been correlated with transcriptional regulation [47,48]. Many studies support the view that G4s are favored by some transcription factors, affecting transcriptional response [49,50]. While several G4 binding proteins were evaluated in animals, including humans, the knowledge of G4-binding proteins in yeast is limited, and the influence of G4s on yeast transcription has not been deeply evaluated.

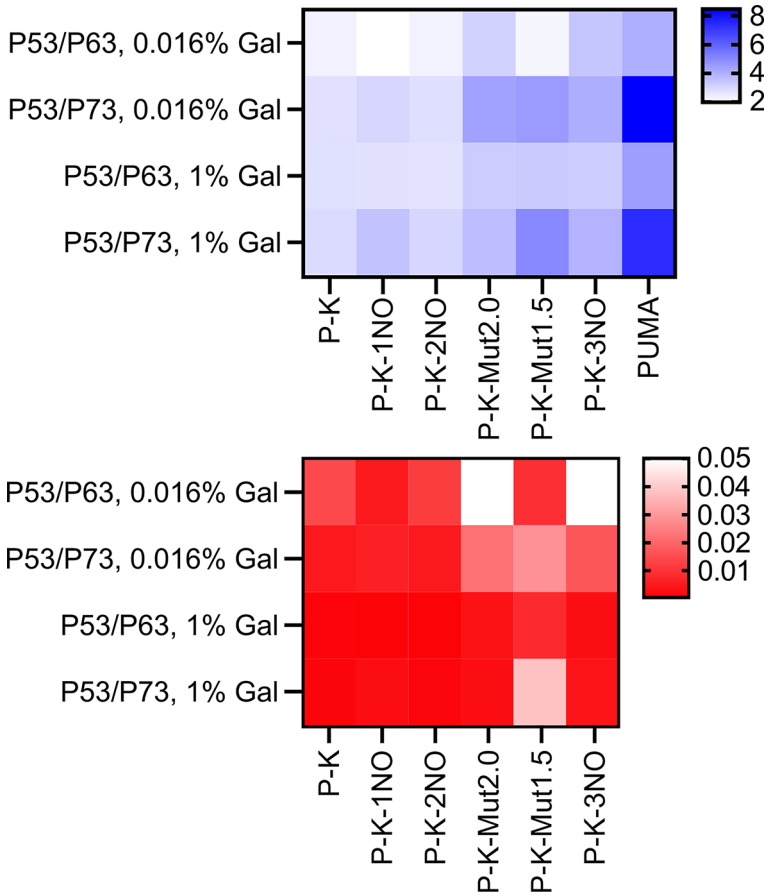

Figure 5. Effect of G4 forming sequences on P53/P63 and P53/P73 relative activity plotted as a heat map

The upper heatmap presents the relative activity of P63 and P73 compared with P53 (shades of blue with the indicated color scale; average of three to six replicates) in *yLFM reporter strains*; the lower heatmap presents the results of multiple unpaired *t*-tests, assuming individual variance for each row and a two-stage step-up method to compare the relative activities measured in the control PUMA strain with strains containing the other G4 regulatory elements (shades of red, *P*-value <0.05; white = not significant.). Data with corresponding statistical analysis were obtained after 6 h of growth in media containing 0.016% or 1% galactose. Data are also presented as bar graphs in Supplementary Figure S4.

In the present study, our objective was to develop a proof-of-concept framework to investigate how features of different G4 prone sequences impact both basal and induced transcription in a defined, isogenic yeast model. While our approach relies on an artificial promoter-reporter construct, it has the advantage of testing defined variants of G4, embedded at the same position in a chromosomal locus upstream of a minimal promoter driving the *LUC1* reporter [25,26]. Further upstream of the G4 motif is a transcription factor RE from the *BBC3* (PUMA) gene that is targeted by P53 family proteins (Supplementary Figure S1). Exploiting a tunable promoter, we were able to obtain results with a defined matrix of variables consisting of (i) six different G4-forming proneness or a control sequence that does not form a G4 structure (i.e., PUMA) (Table 1), and (ii) different levels of P63, P73 or P53 (TA α variant) that differ in their binding affinity to the RE. The choice of P53 family transcription factors to investigate the impact of G4 prone sequences on transactivation was linked to our previous studies in which their transcriptional responses to many different variants of binding sites in the same chromosomal locus and yeast reporter system have been characterized [33]. Contrary to previous studies where one G4-forming sequence (i.e., KSHV) was studied by placing it either upstream or downstream of the P53 response element [25,26], here we investigated how changes in G-quadruplex propensity affect transactivation by exploiting a panel of six isogenic yeast reporter strains (Supplementary Figure S1). Interestingly, our results highlighted that an increase in basal transactivation is correlated with higher G-quadruplex propensity (Figure 6, panel A); this crucial observation was not obvious from previous results. Moreover, the possibility to test the entire family of P53 transcription factor was an added value of our proof-of-concept matrix; in fact,

Bioscience Reports (2023) **43** BSR20231348
https://doi.org/10.1042/BSR20231348

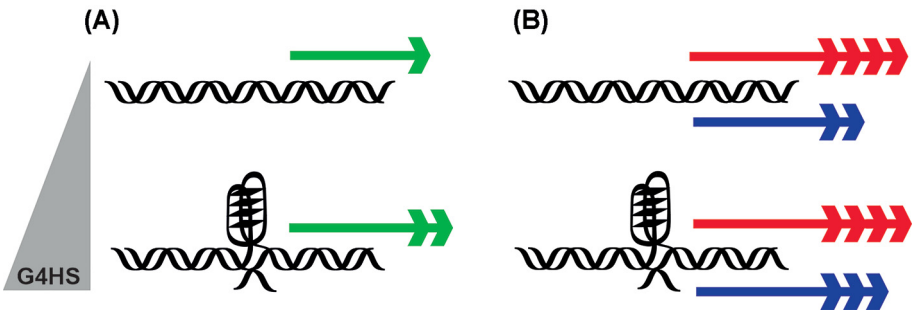

Figure 6. Scheme of G4 influence on yeast transcription

(**A**) Basal transcription (green arrows) correlates with the presence of G-quadruplex forming sequences and an increase in G4 hunter score (G4HS, gray) leads to higher activity of the luciferase-associated yeast minimal promoter. (**B**) P53 family proteins (P53:red arrows; P63/P73:blue arrows) are not equally influenced by the presence of the G-quadruplex forming sequence. The length and number of arrows correspond to the level of transcriptional activity.

P53 family proteins can recognize binding sites with similar but not identical features. Also, the three proteins differ in the strength of transactivation, which is in part related to differences in quaternary structures and the presence of different combinations of domains [22,51,52]. In this regard, the presence of a G4 prone sequence in proximity to the P53 RE seems to support the activity of the weaker P63 and P73 transcription factors, possibly by facilitating their accessibility to the P53 RE or by increasing their interaction with the basal transcription machinery (Figure 6).

Moreover, we chose the PUMA derived RE due to its intermediate transactivation potential, reasoning that it could represent a sensitive tool to monitor the impact of changes in the surrounding sequences [25,33,53]. We have shown previously that high-affinity consensus P53 binding sites lead to high-level transactivation even when P53 protein is kept at minimum levels, preventing the tuning of promoter responses [54,55]. Indeed, the PUMA RE features three mismatches from the optimal P53 consensus site and does not contain the optimal, more flexible, CATG element in the core CWWG motifs; at the same time, it is responsive also to P63 and P73. Lastly, despite the *S. cerevisiae* genome being characterized by a low GC content and a low propensity to adopt G4s [43], a recent study identified 37 genes whose promoter contains a G4 [56]. Moreover, several yeast proteins are able to interact with G4s. Interestingly, binding to G4 DNA was demonstrated for the yeast transcription factor Msn2 with corresponding increased activity, while disruption of the G4 motif led to reduced transactivation [56]; G4 specificity was also shown for Nsr1 and Sub1 yeast proteins [57,58]. Therefore, the defined presence of G4-prone sequences in an isogenic yeast system can serve as a tool to analyze G4-dependent regulation of yeast transcription.

The six G4 sequences selected in the present study were modeled on the positive control sequence derived from the KSHV genome sequence [25]; specific changes were introduced to decrease the propensity to form G4s by the G4 Killer program [27] or by sequential substitution of G bases in guanine repeats. The resulting sequences were classified according to the G4 Hunter algorithm [28], a widely used tool for G4 prediction that takes into account G-richness and G-skewness of DNA or RNA sequences and provides a quadruplex propensity score.

The selected G4-prone sequences were biophysically characterized by ThT assays and CD spectroscopic analyses. ThT is a fluorescent probe that binds G4s more strongly than duplex or single stranded DNA, and for which a procedure for the rapid detection of G4 structures has been developed and verified [59]. Using the ThT assay, we confirmed the formation of G4s not only in the previously analyzed KSHV sequence [25] but also in the oligonucleotides we selected and characterized by a lower G4 Hunter score (Figure 1 and Supplementary Table 1). However, some deviations from the bioinformatic prediction of G4 formation were observed, mainly due to the possibility of parallel G4 formation in short oligonucleotides. Indeed, the value of the G4 Hunter score is based on the number of concurrent G bases (G-runs) and the total length of the sequence. Although the presence of G-runs is essential for G4 formation, differences in bioinformatics-determined PQS (potential quadruplex-forming sequences) and preferences for G4 formation *in vitro* have been demonstrated [60]. The results may have been influenced by the nature of ThT binding to DNA. A significant increase in fluorescence emission can occur due to inhibition of rotation of the ThT inner segments; binding of ThT to different DNA structures leads to different degrees of inhibition of torsional motion [61]. Three different binding modes to DNA have been described for ThT: binding to DNA cavities, intercalation between DNA bases, and external binding to DNA phosphate groups; ThT bound in each mode has a different yield of fluorescence [62].

The results of CD spectroscopy in the presence of potassium confirmed (i) the stabilization of parallel G4 conformation in KSHV, KSHV-1NO, KSHV-2NO oligonucleotides, (ii) an antiparallel conformation in KSHV-Mut1.5 sequence and (iii) a hybrid conformation in KSHV-Mut2.0 motif. That a parallel G4 conformation is represented to a higher extent in KSHV-1NO and KSHV-2NO (Figure 2C,D) than in the positive control KSHV oligonucleotide (Figure 2B), where the positive peak at 295 nm in the CD spectra partially indicates the formation of hybrid G4, is consistent with the results of the ThT assay. Indeed, ThT was reported to possess high specificity for the parallel G4 conformation [63,64]. The change in the G4 conformation of KSHV-Mut1.5 also corresponds to the ThT assay results, where a decrease in fluorescence intensity was observed in the potassium ion environment, indicating ThT binding to the less preferred G4 structure.

Transactivation data in our experimental system indicate that the presence of these G4 prone sequences enhances basal transcription proportional to their potential to form secondary structures (Figure 3). Higher levels of transactivation are also apparent when the transcription rates are enhanced by expression of the sequence-specific P53 family of transcription factors, but in this case an inverse relation to affinity and transactivation potential is evident (Figure 4).

Transcription factor-induced activity is typically expressed in reporter assays as fold change of transactivation, to focus on the direct impact of a trans-factor on gene expression. Considering that the promoter-reporter system used reached a maximal rate of transactivation, the relative fold change due to the P53 family proteins is lower when a G4 prone sequence is embedded near the promoter site, due to the effect of these sequence in increasing the basal, P53-independent transcription. Fold change graphs show a negative impact of G4 prone sequences particularly for P53 (Supplementary Figure S3); indeed, this negative effect is proportional to the G4 Hunter score, with the exception of KSHV-3NO. However, we emphasize that the fold change view is partially misleading, since the presence of G4s increase overall promoter transcription in all cases, particularly the basal activity.

In general, P53 exhibits a much stronger transactivation potential than P73 and P63 as TA α variant in yeast [54,65]. We exploited this feature, along with the inducible and tunable nature of the expression vector, to ask whether the impact of studied G4 prone sequences could be more relevant in cooperating with the weaker transcription factors P63 and P73. This seemed to be the case and led to a significant reduction in the relative activity of P53 over that of P63 and P73 with the presence of G4 forming sequence at the promoter site, and inversely proportional to the G4 Hunter score (Figure 5).

While we have no formal proof that G4 sequences are stably formed at the endogenous yeast locus where they were cloned, the impact of those sequences on transactivation broadly followed the predictions from the G4 Hunter score. However, there were some exceptions, and the KSHV-1NO sequence showed an equivalent or even a slightly higher transactivation compared to the highest-scoring KHSV sequence. This is in part consistent with the results of ThT measurements performed in the presence of KCl. Moreover, the KSHV-3NO sequence showed higher basal transactivation than the higher scoring KSHV-Mut1.5 motif, although *in vitro* experiments did not show a propensity for the former to form G4s. One limitation from our *in-cellulo* approach is represented by the inability to fully understand the contribution of a G4 prone sequence as primary sequence motifs or the effect at the level of local DNA structures. In other words, we cannot exclude that, by replacing the G content with A stretches in the oligonucleotides, new binding sites for yeast resident transcription factors are formed that can lead to higher basal transactivation independently from the formation of a G4 structure.

In conclusion, our proof-of-concept experiment modeled the impact of defined changes in G4 prone sequences at a yeast chromatin locus on both basal and induced transactivation, exploiting a well-established isogenic reporter assay. That local G4 structures influence the functionality of P53 family proteins could have important implications for the functional classification of pathogenic P53 or P63 missense mutant alleles that retain partial transactivation capacity, therefore influencing their relative activity on specific target genes.

Data Availability

All data are available in the article and supplementary materials.

Competing Interests

The authors declare that there are no competing interests associated with the manuscript.

Funding

This work was supported by the Czech Science Foundation [grant number 22-21903S (to V.B.)] and the Italian Ministry of Health 5 × 1000 funds 2020 (to P.M.).

CRediT Author Contribution

Libuše Kratochvilová: Data curation, Formal analysis, Investigation, Writing—original draft. **Matúš Vojsovič:** Data curation, Formal analysis, Investigation. **Natália Valková:** Data curation, Methodology. **Lucie Šislerová:** Validation. **Zeinab El Rashed:** Validation, Investigation, Visualization, Writing—review & editing. **Alberto Inga:** Visualization, Methodology, Writing—original draft, Writing—review & editing. **Paola Monti:** Data curation, Investigation, Visualization, Writing—original draft, Project administration, Writing—review & editing. **Václav Brázda:** Conceptualization, Project administration, Writing—review & editing.

Acknowledgements

The authors thank Philip Coates for critical reading and English proofreading.

Abbreviations

CD, circular dichroism; DBD, DNA-binding domain; G4, G-quadruplex; OD, oligomerization domain; RE, response element; UTR, untranslated region.

References

1 ENCODE Project Consortium (2012) An integrated encyclopedia of DNA elements in the human genome. *Nature* **489**, 57–74, https://doi.org/10.1038/nature11247
2 Teng, F.-Y., Jiang, Z.-Z., Guo, M., Tan, X.-Z., Chen, F., Xi, X.-G. et al. (2021) G-Quadruplex DNA: a novel target for drug design. *Cell. Mol. Life Sci.* **78**, 6557–6583, https://doi.org/10.1007/s00018-021-03921-8
3 Zhang, X., Spiegel, J., Martínez Cuesta, S., Adhikari, S. and Balasubramanian, S. (2021) Chemical profiling of DNA G-quadruplex-interacting proteins in live cells. *Nat. Chem.* **13**, 626–633, https://doi.org/10.1038/s41557-021-00736-9
4 Kolesnikova, S. and Curtis, E.A. (2019) Structure and function of multimeric G-quadruplexes. *Molecules* **24**, 3074, https://doi.org/10.3390/molecules24173074
5 Mendoza, O., Bourdoncle, A., Boulé, J.-B., Brosh, R.M. and Mergny, J.-L. (2016) G-quadruplexes and helicases. *Nucleic Acids Res.* **44**, 1989–2006, https://doi.org/10.1093/nar/gkw079
6 Brázda, V., Hároníková, L., Liao, J.C.C. and Fojta, M. (2014) DNA and RNA quadruplex-binding proteins. *Int. J. Mol. Sci.* **15**, 17493–17517, https://doi.org/10.3390/ijms151017493
7 Li, G., Su, G., Wang, Y., Wang, W., Shi, J., Li, D. et al. (2023) Integrative genomic analyses of promoter G-quadruplexes reveal their selective constraint and association with gene activation. *Commun Biol* **6**, 625, https://doi.org/10.1038/s42003-023-05015-6
8 Shu, H., Zhang, R., Xiao, K., Yang, J. and Sun, X. (2022) G-quadruplex-binding proteins: promising targets for drug design. *Biomolecules* **12**, 648, https://doi.org/10.3390/biom12050648
9 Varshney, D., Spiegel, J., Zyner, K., Tannahill, D. and Balasubramanian, S. (2020) The regulation and functions of DNA and RNA G-quadruplexes. *Nat. Rev. Mol. Cell Biol.* **21**, 459–474, https://doi.org/10.1038/s41580-020-0236-x
10 Simonsson, T., Pecinka, P. and Kubista, M. (1998) DNA tetraplex formation in the control region of C-Myc. *Nucleic Acids Res.* **26**, 1167–1172, https://doi.org/10.1093/nar/26.5.1167
11 Siddiqui-Jain, A., Grand, C.L., Bearss, D.J. and Hurley, L.H. (2002) Direct evidence for a G-quadruplex in a promoter region and its targeting with a small molecule to repress c-MYC transcription. *Proc. Natl. Acad. Sci.* **99**, 11593–11598, https://doi.org/10.1073/pnas.182256799
12 Cogoi, S. and Xodo, L.E. (2006) G-quadruplex formation within the promoter of the KRAS proto-oncogene and its effect on transcription. *Nucleic Acids Res.* **34**, 2536–2549, https://doi.org/10.1093/nar/gkl286
13 Bejugam, M., Sewitz, S., Shirude, P.S., Rodriguez, R., Shahid, R. and Balasubramanian, S. (2007) Trisubstituted isoalloxazines as a new class of G-quadruplex binding ligands: small molecule regulation of c-kit oncogene expression. *J. Am. Chem. Soc.* **129**, 12926–12927, https://doi.org/10.1021/ja075881p
14 Chen, L., Dickerhoff, J., Sakai, S. and Yang, D. (2022) DNA G-quadruplex in human telomeres and oncogene promoters: structures, functions, and small molecule targeting. *Acc. Chem. Res.* **55**, 2628–2646, https://doi.org/10.1021/acs.accounts.2c00337
15 Bahls, B., Aljnadi, I.M., Emídio, R., Mendes, E. and Paulo, A. (2023) G-quadruplexes in c-MYC promoter as targets for cancer therapy. *Biomedicines* **11**, 969, https://doi.org/10.3390/biomedicines11030969
16 Zawacka-Pankau, J.E. (2022) The role of P53 family in cancer. *Cancers (Basel)* **14**, 823, https://doi.org/10.3390/cancers14030823
17 Kastenhuber, E.R. and Lowe, S.W. (2017) Putting P53 in context. *Cell* **170**, 1062–1078, https://doi.org/10.1016/j.cell.2017.08.028
18 Boutelle, A.M. and Attardi, L.D. (2021) P53 and tumor suppression: it takes a network. *Trends Cell Biol.* **31**, 298–310, https://doi.org/10.1016/j.tcb.2020.12.011
19 Marcel, V., Dichtel-Danjoy, M.-L., Sagne, C., Hafsi, H., Ma, D., Ortiz-Cuaran, S. et al. (2011) Biological functions of P53 isoforms through evolution: lessons from animal and cellular models. *Cell Death Differ.* **18**, 1815–1824, https://doi.org/10.1038/cdd.2011.120
20 Zhao, L. and Sanyal, S. (2022) P53 isoforms as cancer biomarkers and therapeutic targets. *Cancers (Basel)* **14**, 3145, https://doi.org/10.3390/cancers14133145
21 Bourdon, J.-C. *p53 Family Isoforms. Curr. Pharm. Biotechnol.*, http://www.eurekaselect.com/66037/articleaccessed 2020-04-05), https://doi.org/10.2174/138920107783018444
22 Osterburg, C. and Dötsch, V. (2022) Structural diversity of P63 and P73 isoforms. *Cell Death Differ.* **29**, 921–937, https://doi.org/10.1038/s41418-022-00975-4

23 el-Deiry, W.S., Kern, S.E., Pietenpol, J.A., Kinzler, K.W. and Vogelstein, B. (1992) Definition of a consensus binding site for P53. *Nat. Genet.* **1**, 45–49, https://doi.org/10.1038/ng0492-45
24 Senitzki, A., Safieh, J., Sharma, V., Golovenko, D., Danin-Poleg, Y., Inga, A. et al. (2021) The complex architecture of P53 binding sites. *Nucleic Acids Res.* **49**, 1364–1382, https://doi.org/10.1093/nar/gkaa1283
25 Porubiaková, O., Bohálová, N., Inga, A., Vadovičová, N., Coufal, J., Fojta, M. et al. (2019) The influence of quadruplex structure in proximity to P53 target sequences on the transactivation potential of P53 alpha isoforms. *Int. J. Mol. Sci.* **21** (1), 127, https://doi.org/10.3390/ijms21010127
26 Monti, P., Brazda, V., Bohálová, N., Porubiaková, O., Menichini, P., Speciale, A. et al. (2021) Evaluating the influence of a G-quadruplex prone sequence on the transactivation potential by wild-type and/or mutant P53 family proteins through a yeast-based functional assay. *Genes (Basel)* **12**, 277, https://doi.org/10.3390/genes12020277
27 Brazda, V., Kolomaznik, J., Mergny, J.-L. and Stastny, J. (2020) G4Killer web application: a tool to design G-quadruplex mutations. *J. Bioinform.* **36** (10), 3246–3247, https://doi.org/10.1093/bioinformatics/btaa057
28 Bedrat, A., Lacroix, L. and Mergny, J.-L. (2016) Re-evaluation of G-quadruplex propensity with G4Hunter. *Nucleic Acids Res.* **44**, 1746–1759, https://doi.org/10.1093/nar/gkw006
29 Renaud de la Faverie, A., Guédin, A., Bedrat, A., Yatsunyk, L.A. and Mergny, J.-L. (2014) Thioflavin T as a fluorescence light-up probe for G4 formation. *Nucleic Acids Res.* **42**, e65, https://doi.org/10.1093/nar/gku111
30 Harrel Jr., W.A. (2006) *Quadruplex Nucleic Acids* (Neidle, S. and Balasubramanian, S., eds), Royal Society of Chemistry, https://doi.org/10.1039/9781847555298
31 Biffi, G., Tannahill, D., McCafferty, J. and Balasubramanian, S. (2013) Quantitative visualization of DNA G-quadruplex structures in human cells. *Nat. Chem.* **5**, 182–186, https://doi.org/10.1038/nchem.1548
32 Storici, F. and Resnick, M.A. (2003) Delitto perfetto targeted mutagenesis in yeast with oligonucleotides. *Genet. Eng. (N. Y.)* **25**, 189–207
33 Inga, A., Storici, F., Darden, T.A. and Resnick, M.A. (2002) Differential transactivation by the P53 transcription factor is highly dependent on P53 level and promoter target sequence. *Mol. Cell. Biol.* **22**, 8612–8625, https://doi.org/10.1128/MCB.22.24.8612-8625.2002
34 Monti, P., Ciribilli, Y., Bisio, A., Foggetti, G., Raimondi, I., Campomenosi, P. et al. (2014) ΔN-P63α and TA-P63α exhibit intrinsic differences in transactivation specificities that depend on distinct features of DNA target sites. *Oncotarget* **5**, 2116–2130, https://doi.org/10.18632/oncotarget.1845
35 Monti, P., Bosco, B., Gomes, S., Saraiva, L., Fronza, G. and Inga, A. (2019) Yeast as a chassis for developing functional assays to study human P53. *JoVE (J. Visualized Experiments)* **150**, e59071
36 Kejnovská, I., Renčiuk, D., Palacký, J. and Vorlíčková, M. (2019) CD Study of the G-Quadruplex Conformation. *Methods Mol. Biol.* **2035**, 25–44, https://doi.org/10.1007/978-1-4939-9666-7˙2
37 Lambert, S.A., Jolma, A., Campitelli, L.F., Das, P.K., Yin, Y., Albu, M. et al. (2018) The human transcription factors. *Cell* **172**, 650–665, https://doi.org/10.1016/j.cell.2018.01.029
38 Rube, H.T., Rastogi, C., Kribelbauer, J.F. and Bussemaker, H.J. (2018) A unified approach for quantifying and interpreting DNA shape readout by transcription factors. *Mol. Syst. Biol.* **14**, e7902, https://doi.org/10.15252/msb.20177902
39 Schnepf, M., von Reutern, M., Ludwig, C., Jung, C. and Gaul, U. (2020) Transcription factor binding affinities and DNA shape readout. *iScience* **23**, 101694, https://doi.org/10.1016/j.isci.2020.101694
40 Zhou, T., Shen, N., Yang, L., Abe, N., Horton, J., Mann, R.S. et al. (2015) Quantitative modeling of transcription factor binding specificities using DNA shape. *Proc. Natl. Acad. Sci. U.S.A.* **112**, 4654–4659, https://doi.org/10.1073/pnas.1422023112
41 Brázda, V., Bartas, M. and Bowater, R.P. (2021) Evolution of diverse strategies for promoter regulation. *Trends Genet.* **37**, 730–744, https://doi.org/10.1016/j.tig.2021.04.003
42 Spiegel, J., Adhikari, S. and Balasubramanian, S. (2020) The structure and function of DNA G-quadruplexes. *Trends Chem.* **2**, 123–136, https://doi.org/10.1016/j.trechm.2019.07.002
43 Čutová, M., Manta, J., Porubiaková, O., Kaura, P., Šťastný, J., Jagelská, E.B. et al. (2020) Divergent distributions of inverted repeats and G-quadruplex forming sequences in Saccharomyces cerevisiae. *Genomics* **112**, 1897–1901, https://doi.org/10.1016/j.ygeno.2019.11.002
44 Hänsel-Hertsch, R., Di Antonio, M. and Balasubramanian, S. (2017) DNA G-quadruplexes in the human genome: detection, functions and therapeutic potential. *Nat. Rev. Mol. Cell Biol.* **18**, 279–284, https://doi.org/10.1038/nrm.2017.3
45 Bohálová, N., Mergny, J.-L. and Brázda, V. (2021) Novel G-quadruplex prone sequences emerge in the complete assembly of the human X chromosome. *Biochimie* **191**, 87–90, https://doi.org/10.1016/j.biochi.2021.09.004
46 Hennecker, C., Yamout, L., Zhang, C., Zhao, C., Hiraki, D., Moitessier, N. et al. (2022) Structural polymorphism of guanine quadruplex-containing regions in human promoters. *Int. J. Mol. Sci.* **23**, 16020, https://doi.org/10.3390/ijms232416020
47 Brázda, V., Kolomazník, J., Lýsek, J., Bartas, M., Fojta, M., Šťastný, J. et al. (2019) G4Hunter Web application: a web server for G-quadruplex prediction. *Bioinformatics* **35**, 3493–3495, https://doi.org/10.1093/bioinformatics/btz087
48 Nadai, M. and Richter, S.N. (2019) G-quadruplex visualization in cells via antibody and fluorescence probe. *Methods Mol. Biol.* **2035**, 383–395, https://doi.org/10.1007/978-1-4939-9666-7˙24
49 Lago, S., Nadai, M., Cernilogar, F.M., Kazerani, M., Domíniguez Moreno, H., Schotta, G. et al. (2021) Promoter G-quadruplexes and transcription factors cooperate to shape the cell type-specific transcriptome. *Nat. Commun.* **12**, 3885, https://doi.org/10.1038/s41467-021-24198-2
50 Spiegel, J., Cuesta, S.M., Adhikari, S., Hänsel-Hertsch, R., Tannahill, D. and Balasubramanian, S. (2021) G-quadruplexes are transcription factor binding hubs in human chromatin. *Genome Biol.* **22**, 117, https://doi.org/10.1186/s13059-021-02324-z
51 Joerger, A.C. and Fersht, A.R. (2016) The P53 pathway: origins, inactivation in cancer, and emerging therapeutic approaches. *Annu. Rev. Biochem.* **85**, 375–404, https://doi.org/10.1146/annurev-biochem-060815-014710
52 Belyi, V.A., Ak, P., Markert, E., Wang, H., Hu, W., Puzio-Kuter, A. et al. (2010) The origins and evolution of the P53 family of genes. *Cold Spring Harb. Perspect. Biol.* **2**, a001198, https://doi.org/10.1101/cshperspect.a001198

53 Menendez, D., Inga, A. and Resnick, M.A. (2009) The Expanding Universe of P53 Targets. *Nat. Rev. Cancer* **9**, 724–737, https://doi.org/10.1038/nrc2730

54 Ciribilli, Y., Monti, P., Bisio, A., Nguyen, H.T., Ethayathulla, A.S., Ramos, A. et al. (2013) Transactivation specificity is conserved among P53 family proteins and depends on a response element sequence code. *Nucleic Acids Res.* **41**, 8637–8653, https://doi.org/10.1093/nar/gkt657

55 Tebaldi, T., Zaccara, S., Alessandrini, F., Bisio, A., Ciribilli, Y. and Inga, A. (2015) Whole-genome cartography of P53 response elements ranked on transactivation potential. *BMC Genomics* **16**, 464, https://doi.org/10.1186/s12864-015-1643-9

56 Duy, D.L. and Kim, N. (2023) Yeast transcription factor Msn2 binds to G4 DNA. *Nucleic. Acids. Res.* **51**, 9643–9657, https://doi.org/10.1093/nar/gkad684

57 Singh, S., Berroyer, A., Kim, M. and Kim, N. (2020) Yeast Nucleolin Nsr1 impedes replication and elevates genome instability at an actively transcribed guanine-rich G4 DNA-forming sequence. *Genetics* **216**, 1023–1037, https://doi.org/10.1534/genetics.120.303736

58 Gao, J., Zybailov, B.L., Byrd, A.K., Griffin, W.C., Chib, S., Mackintosh, S.G. et al. (2015) Yeast transcription co-activator sub1 and its human homolog PC4 preferentially bind to G-quadruplex DNA. *Chem. Commun. (Camb.)* **51**, 7242–7244, https://doi.org/10.1039/C5CC00742A

59 Krämer, J., Kang, R., Grimm, L.M., De Cola, L., Picchetti, P. and Biedermann, F. (2022) Molecular probes, chemosensors, and nanosensors for optical detection of biorelevant molecules and ions in aqueous media and biofluids. *Chem. Rev.* **122**, 3459–3636, https://doi.org/10.1021/acs.chemrev.1c00746

60 Lages, A., Proud, C.G., Holloway, J.W. and Vorechovsky, I. (2019) Thioflavin T monitoring of guanine quadruplex formation in the Rs689-dependent INS Intron 1. *Mol. Ther. Nucleic Acids* **16**, 770–777, https://doi.org/10.1016/j.omtn.2019.04.026

61 Stsiapura, V.I., Maskevich, A.A., Kuzmitsky, V.A., Uversky, V.N., Kuznetsova, I.M. and Turoverov, K.K. (2008) Thioflavin T as a molecular rotor: fluorescent properties of thioflavin T in solvents with different viscosity. *J. Phys. Chem. B* **112**, 15893–15902, https://doi.org/10.1021/jp805822c

62 Hanczyc, P., Rajchel-Mieldzioć, P., Feng, B. and Fita, P. (2021) Identification of thioflavin T binding modes to DNA: a structure-specific molecular probe for lasing applications. *J. Phys. Chem. Lett.* **12**, 5436–5442, https://doi.org/10.1021/acs.jpclett.1c01254

63 Bugaut, A. and Balasubramanian, S. (2012) 5′-UTR RNA G-quadruplexes: translation regulation and targeting. *Nucleic Acids Res.* **40**, 4727–4741, https://doi.org/10.1093/nar/gks068

64 Joachimi, A., Benz, A. and Hartig, J.S. (2009) A Comparison of DNA and RNA quadruplex structures and stabilities. *Bioorg. Med. Chem.* **17**, 6811–6815, https://doi.org/10.1016/j.bmc.2009.08.043

65 Monti, P., Ciribilli, Y., Bisio, A., Foggetti, G., Raimondi, I., Campomenosi, P. et al. (2014) ΔN-P63α and TA-P63α exhibit intrinsic differences in transactivation specificities that depend on distinct features of DNA target sites. *Oncotarget* **5**, 2116–2130, https://doi.org/10.18632/oncotarget.1845

The presence of a G4 prone sequence upstream of a minimal promoter increases transcriptional activity in the yeast *S. cerevisiae*

Supplementary Figures and legends

Libuše Kratochvilová, Matúš Vojsovič, Natália Valková, Lucie Šislerová, Zeinab El Rashed, Alberto Inga, Paola Monti, Václav Brázda[§]

§Corresponding author:

Václav Brázda

Institute of Biophysics of the Czech Academy of Sciences, Královopolská 135, 61265 Brno, Czech Republic

vaclav@ibp.cz

Oligonucleotides	$I_{(0)}$ Tris-HCl	$I_{(KCl)}$ Tris-HCl + 100mM KCl	$I_{(KCl)}/I_{(0)}$
PUMA	1.75 ± 0.23	1.39 ± 0.04	↓ 0.79
KSHV	16.93 ± 0,08	19.22 ± 0.38	↑ 1.14
KSHV-1NO	25.36 ± 0.12	31.76 ± 0.44	↑ 1.25
KSHV-2NO	9.73 ± 0.61	25.69 ± 0.76	↑ 2.64
KSHV-Mut2.0	19.87 ± 0.87	23.89 ± 1.40	↑ 1.20
KSHV-Mut1.5	15.24 ± 1.20	10.14 ± 0.15	↓ 0,67
KSHV-3NO	6.98 ± 0.92	10.58 ± 0.73	↑ 1.51

Table S1. Fluorescence intensity I/I_0 determined from oligonucleotides with the potential to form G4s. The average fluorescence intensity of three repetitions was related to the fluorescence intensity of the blank (ThT with the appropriate buffer). The $I_{(KCl)}/I_{(0)}$ fold indicates the fold decrease (↓) or increase (↑) of fluorescence emission of samples in buffer with the addition of K+ ions compared to samples in Tris-HCl without KCl.

Figure S1. Sequence of the *ADE2* chromosomal locus edited to build the luciferase-based reporter assay. The *S. cerevisiae ADE2* locus on chromosomal XV was engineered as follows: first the *ADE2* open reading frame was replaced with the *Pothinus pyralis* firefly cDNA open reading frame (yellow annotation, the first ~70 nts are shown); concomitantly the *ADE2* promoter was replaced by a 245 nt portion of the promoter of the *CYC1* gene, corresponding to the sequence naturally present in chromosome X, from nucleotide 526090 till nucleotide 526335 (blue annotation) (Inga. 2022, ref 33). This sequence provides for low-level basal transcription of the luciferase gene. The locus has been further modified by placing upstream of the minimal CYC1 promoter the P53 RE derived from the human PUMA gene (hsPUMA p53 RE, green annotation) (Porubiakova, 2019, ref 25). Finally, for the experiments presented in this study, we constructed and used a panel of strains that differ only for the presence of a G4 prone sequence (purple annotation, the asterisk indicates that the KSHV is one of six elements that were tested, whose sequences are presented in Table 1) . The correct editing of the locus was confirmed by colony PCR and Sanger sequencing (see the Methods section for further details on the strain construction).

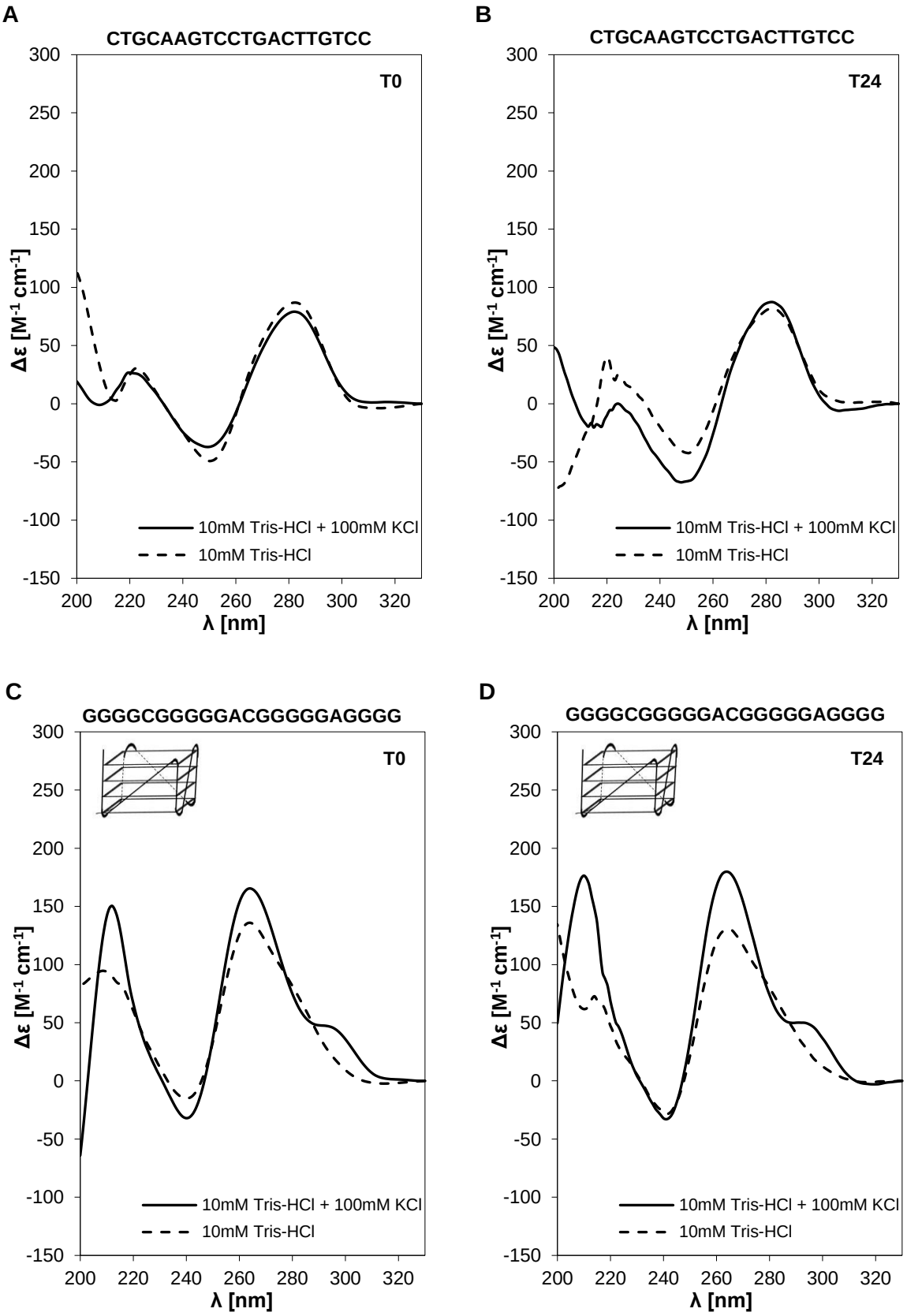
A
CTGCAAGTCCTGACTTGTCC
T0
Δε [M-1 cm-1]
λ [nm]
10mM Tris-HCl + 100mM KCl
10mM Tris-HCl
B
CTGCAAGTCCTGACTTGTCC
T24
Δε [M-1 cm-1]
λ [nm]
10mM Tris-HCl + 100mM KCl
10mM Tris-HCl
C
GGGGCGGGGGACGGGGGAGGGG
T0
Δε [M-1 cm-1]
λ [nm]
10mM Tris-HCl + 100mM KCl
10mM Tris-HCl
D
GGGGCGGGGGACGGGGGAGGGG
T24
Δε [M-1 cm-1]
λ [nm]
10mM Tris-HCl + 100mM KCl
10mM Tris-HCl

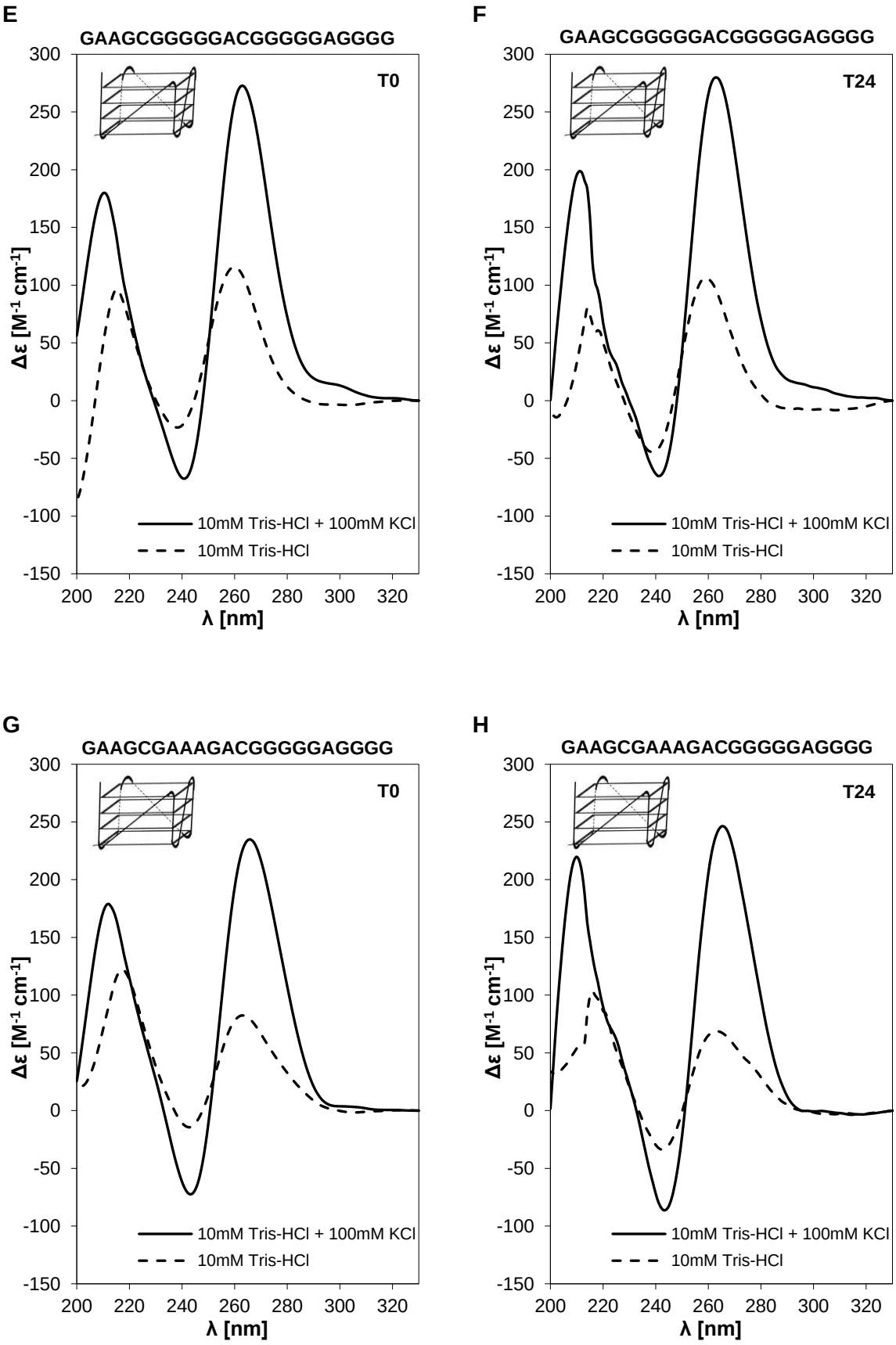
E
GAAGCGGGGGACGGGGGAGGGG
T0
F
GAAGCGGGGGACGGGGGAGGGG
T24
G
GAAGCGAAAGACGGGGGAGGGG
T0
H
GAAGCGAAAGACGGGGGAGGGG
T24
Δε [M-1 cm-1]
λ [nm]
10mM Tris-HCl + 100mM KCl
10mM Tris-HCl

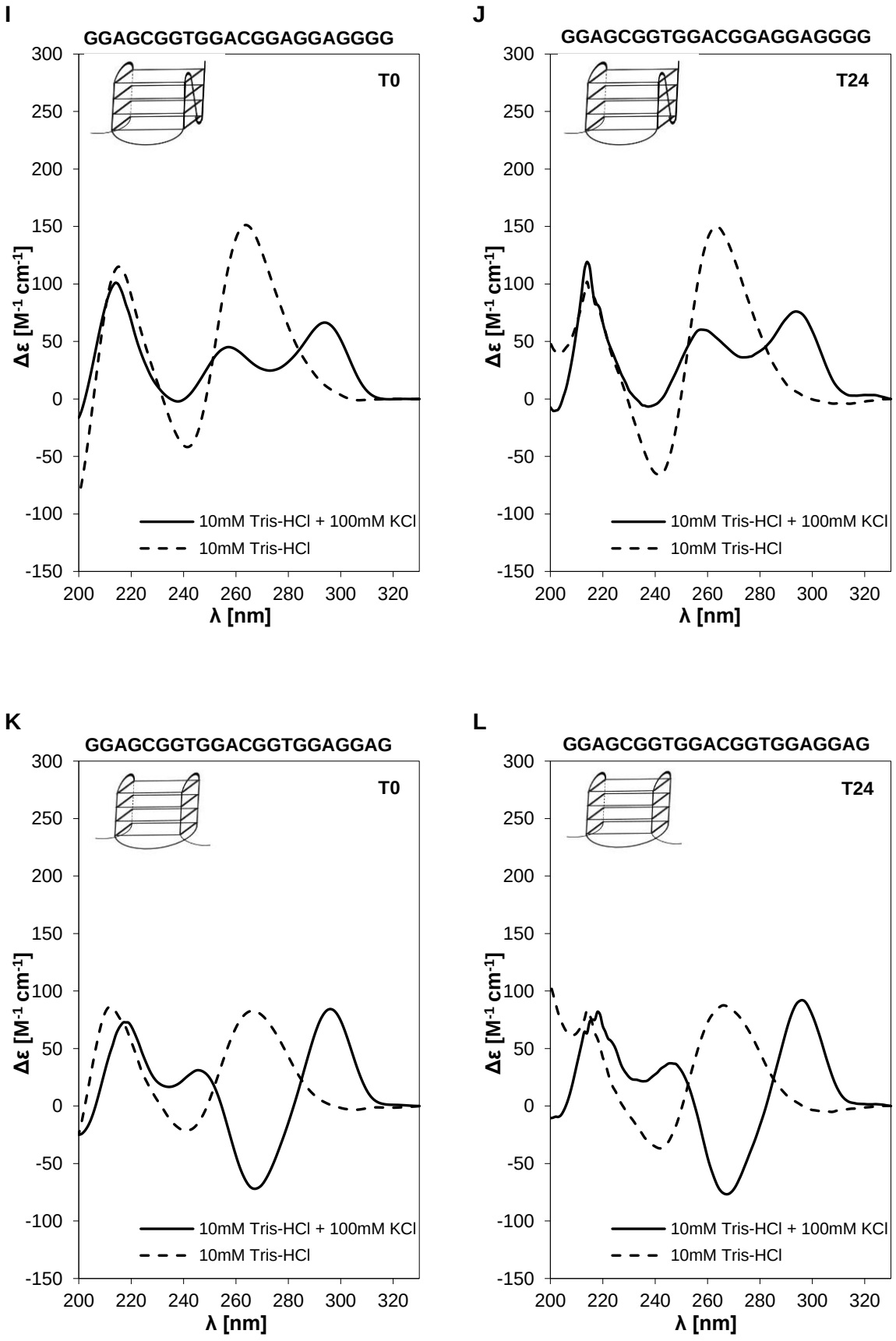
I
GGAGCGGTGGACGGAGGAGGGG
T0
J
GGAGCGGTGGACGGAGGAGGGG
T24
K
GGAGCGGTGGACGGTGGAGGAG
T0
L
GGAGCGGTGGACGGTGGAGGAG
T24
Δε [M-1 cm-1]
λ [nm]
10mM Tris-HCl + 100mM KCl
10mM Tris-HCl

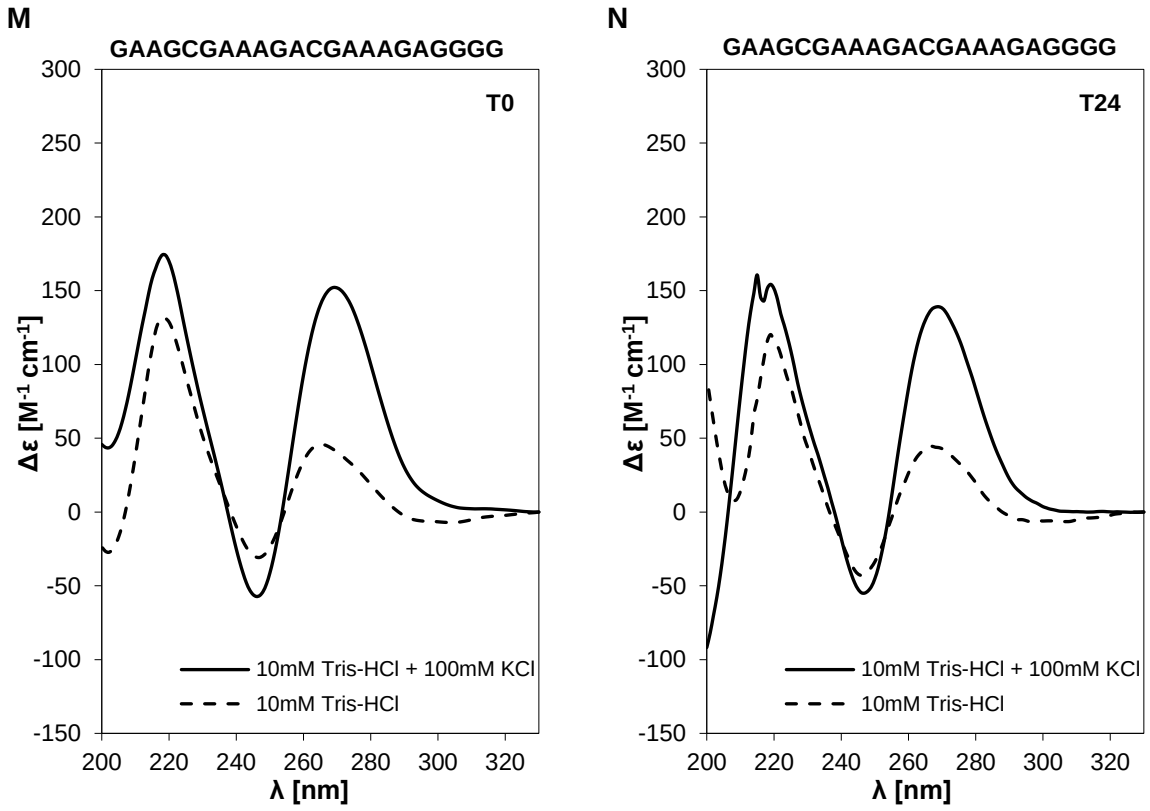

Figure S2. CD spectra of oligonucleotides under study at T_0 (left panel) and T_{24} (right panel). CD spectra of PUMA oligonucleotide **(A, B)**, KSHV oligonucleotide **(C, D)**, KSHV-1NO oligonucleotide **(E, F)**, KSHV-2NO oligonucleotide **(G, H)**, KSHV-Mut2.0 oligonucleotide **(I, J)**, KSHV-Mut1.5 oligonucleotide **(K, L)** and KSHV-3NO oligonucleotide **(M, N)**. The solid line shows the spectra of the sample hybridized in 10 mM Tris-HCl with the addition of 100 mM KCl. The spectra of the sample hybridized in the medium without the addition of K^+ ions are plotted as a dashed line. The CD spectra at T0 from Figure 2 were also reproduced here to facilitate comparisons between the two time points.

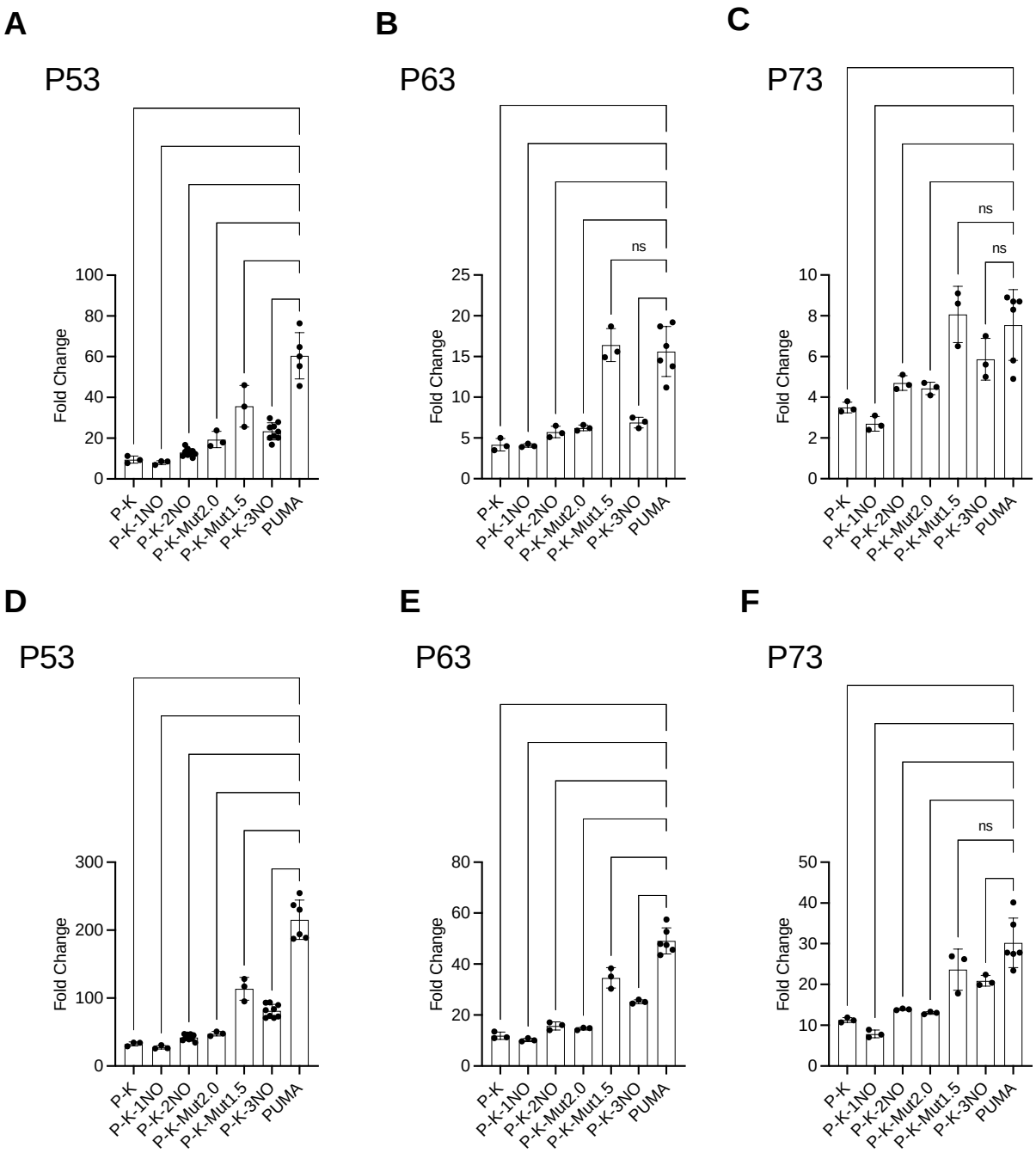

Figure S3. Effect of G4 prone sequences on P53 family transactivation. Fold change measurements for the indicated panel of yLFM reporter strains from P53, P63 and P73 yeast transformants at 0.016% galactose for 6 hours **(A-C)** or at 1% galactose for 6 hours (**D-F**)**.** Data are presented as mean ± standard deviation (SD) of at least three biological replicates. Individual values are also plotted. The symbols *, **, *** and **** indicate significant differences for p*≤0.0146*, p=0.0065, p=0.0006 and p<0.0001, respectively between PUMA strain and those containing other G4 regulatory elements. ns, not significant. Ordinary one-way ANOVA test.

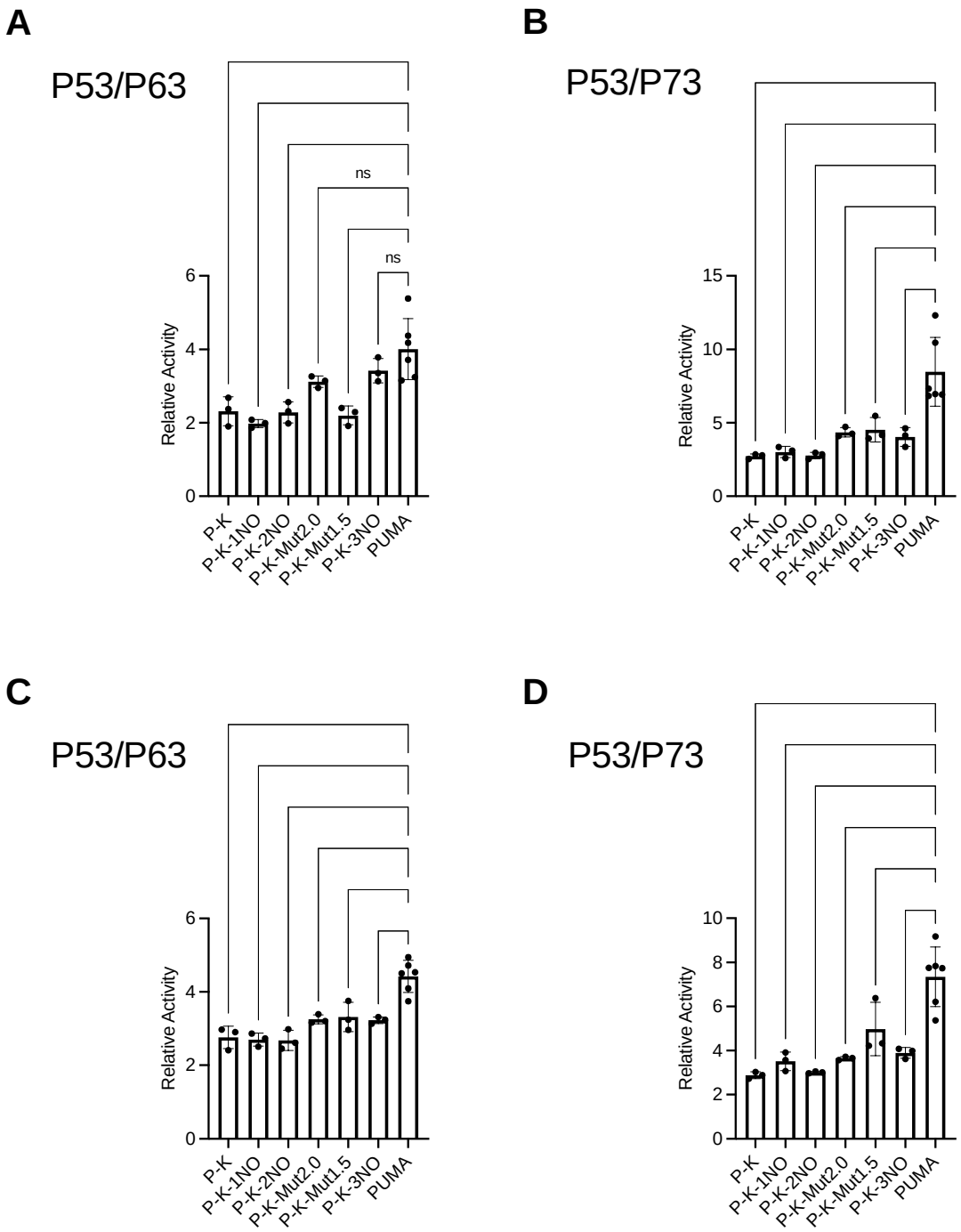

Figure S4. Effect of G4 forming sequences on P53/P63 and P53/P73 relative activity plotted as bars graph. (A), **(C)** P53/P63 relative activity at 0.016% and 1% Galactose, respectively in the indicated panel of yLFM reporter strains. **(B)**, **(D)** P53/P73 relative activity at 0.016% and 1% Galactose, respectively as above. Data are presented as mean ± standard deviation (SD) of at least three biological replicates. Individual values are also plotted. The symbols **, *** and **** indicate significant differences for p*≤0.0064*, p=0.0009, and p<0.0001, respectively between PUMA strain and those containing other G4 regulatory elements. ns, not significant. Ordinary one-way ANOVA test.